



A framework for visual comparison of scalar fields with uncertainty

Viktor Leonhardt¹ · Alexander Wiebel² · Christoph Garth¹

Accepted: 24 September 2024
© The Author(s) 2024

Abstract

Scientists working with uncertain data, such as climate simulations, medical images, or ensembles of physical simulations, regularly confront the problem of comparing observations, e.g., to identify similarities, differences, or patterns. Current approaches in comparative visualization of uncertain scalar fields mainly rely on juxtaposition of both data and uncertainties, where each is represented using, e.g., color mapping or volume rendering. While interpretation of uncertain scalar data from visual encodings is already cognitively challenging, comparison of uncertain fields without explicit visualization support adds a further layer of complexity. In this paper, we present a theoretical framework to devise and describe a class of techniques that directly visualize differences between two or more uncertain scalar fields in a single image. We model each such technique as a combination of one or more interpolation stages, with the application of distance measures on random variables to the resulting distributions, and an appropriate visual encoding. Our framework captures existing methods and lends itself well to formulating new comparative visualization techniques for uncertain data for different visualization scenarios. Furthermore, by modeling uncertain scalar field differences as random variables themselves, we enable additional opportunities for comparison. We demonstrate the usefulness of our framework and its properties by applying it to effective comparative visualization techniques for several synthetic and real-world data sets.

Keywords Uncertainty visualization · Comparative visualization · Ensembles · Visualization framework

1 Introduction

The integration of uncertainties into data models is a common technique in the field of scientific research. A prominent analytical challenge commonly encountered by researchers involves the comparison of uncertain data, e. g., in the research domains of meteorology [43], high-energy physics [15], computational fluid dynamics [19], and medi-

cal science [34]. Although there are existing purely statistical tools designed for the comparison of uncertain data [5], visualization plays a pivotal role in effectively presenting and exploring intricate data sets. To effectively tackle this challenge, researchers require robust tools capable of conducting comprehensive comparative analyses. Visualization stands as a crucial element in unraveling insights from complex data sets. Harnessing the power of comparative visualization methods can significantly augment researchers' ability to delve into uncertain data, uncover patterns, and extract valuable insights. As a result, Kamal et al. [21] suggested comparative uncertainty visualization as a future research direction. Throughout our literature research (cf. Sect. 2), we identified that the current work on visualizations in explicit encoding lacks methods to directly visualize the difference between two or more scalar fields with uncertainty. These studies have mostly focused on the comparison of distinct features. However, a comparison of the entire data set in explicit encoding is a useful method for visualizing subtle differences [32].

This paper presents a theoretical framework for describing a class of techniques for directly comparing between scalar fields with uncertainty, which allows to quickly identify dis-

Alexander Wiebel and Christoph Garth have contributed equally to this work

✉ Viktor Leonhardt
viktor.leonhardt@rptu.de

Alexander Wiebel
wiebel@hs-worms.de

Christoph Garth
garth@rptu.de

¹ Department of Computer Science, RPTU
Kaiserslautern-Landau, Gottlieb-Daimler-Str., Kaiserslautern,
Rheinland-Pfalz 67663, Germany

² Department of Computer Science, Hochschule
WormsUniversity of Applied Sciences, Erenburgerstr. 19,
Worms, Rheinland-Pfalz 67549, Germany

/similarities. Existing methods can be understood in the three steps of the framework. The steps and methods fit well into the parts of established models of the overall visualization pipeline [18, 55]. The framework helps to think and reason about the visual comparison of scalar fields with uncertainty using the explicit encoding paradigm. To evaluate the usefulness of the framework we discuss existing methods in the context of the framework. In addition to other insights, the discussion leads to an additional contribution of the paper by indicating a gap in the research. We make a first step toward closing this gap—visualization of uncertain distances—by implementing a first basic method for this comparison. More research for a very expressive visualization is needed here.

We demonstrate the idea of the proposed framework using a synthetic scalar field with uncertainty. By applying our framework to real-world data sets, we explain how to use it to create comparative visualizations with uncertainties. By supporting the generation of dense comparative visualizations in the *explicit encoding* design [13], this framework serves as a blueprint for producing initial overview visualizations steering further exploration of the comparison of data with uncertainty. Our contributions to the field of comparative uncertainty visualization are the following:

- Proposal of a framework for comparative uncertainty visualization employing statistical and probabilistic distance functions to encode relevant relationships.
- Categorization of the upsampling methods and distance measures incorporated within this framework and analysis of their impact on the resultant visualization.
- The practical implementation of instances of this framework on authentic data sets, encompassing real-world comparison scenarios.

In Sect. 2, we summarize the related work on comparative visualizations with uncertainties and give a brief overview of the three methodological sub-fields it is built on. This section is followed by the main contribution, the definition of the framework, and a classification of the employed methods (distance measures and upsampling methods). Section 5 presents instances of this framework on synthetic and real-world data sets. Further, Sect. 6 is a best-practice guide to allow creating the reader its own comparative uncertainty visualizations. This article then continues in Sect. 7 with a discussion of the framework and a summary of its limitations. Finally, this article concludes the proposed framework in Sect. 8.

2 Related work

The goal of comparative visualization techniques is to identify similarities or dissimilarities between different data sets.

Gleicher et al. [13] defined a taxonomy for this task that is not based on the chart type but on three layout strategies that allow the grouping of existing methods: *superposition*, *juxtaposition*, and *explicit encoding*. These categories also apply to the visual comparisons of uncertain or ensemble data. LYi et al. [32] further refined this taxonomy through a systematic review. Notable surveys that mostly follow this taxonomy have been published for meteorology [43], ensemble data [57], spatial 3D and 4D data [24], and multifaceted scientific data [23]. For our review of state-of-the-art methods, we incorporated research focused on ensemble comparisons. This is a common method for analyzing an unknown distribution because ensembles can be seen as samples from an unknown distribution. This has been applied in research areas such as meteorology [43] and modeling of real-world phenomena through computer simulation models [57].

Juxtaposition is a commonly used visualization design presenting visualizations in a side-by-side view to compare them to each other. This technique uses the user's cognitive capabilities to identify differences and similarities. Its frequent usage can be attributed to its simplicity and straightforward implementation which is applied by many authors to compare their methods to others, e. g. [31, 39, 42]. Furthermore, authors favor the juxtaposition layout because it preserves the original visualization, enabling the presentation of novel methods while also serving as a component in the comparison with other methods. However, it is important to note that comparing complex data using this design layout can be a tedious task. This is especially true for the identifications of subtle differences while concurrently interpreting them.

Superposition reduces the cognitive load of the user through presenting the data in aligned positions. Thus, an implicit mental registration of the presented scenes, like in the juxtaposition, is now explicit in the visualization. This allows for a "quick and easy" comparison [10] since the pertinent visual elements are closely arranged, which probes particularly advantageous when the emphasis lies in spatial disparity comparison. However, a significant drawback of this layout is the potential for visual interference, subsequently giving rise to scalability challenges. This can escalate especially when multiple data attributes are superimposed resulting in visual clutter.

Explicit encoding transforms two or several pieces of information into one desired characteristic quantity, which is then visualized. This is achieved through metrics, which allow the explicit comparison of the data to a desired relationship. This eliminates the need for the viewer to engage in a cognitive comparison or seek out differences, as these have already been computed. Such an approach is particularly advantageous when the focus is on discerning subtle disparities [28]. However, while applying solely this design

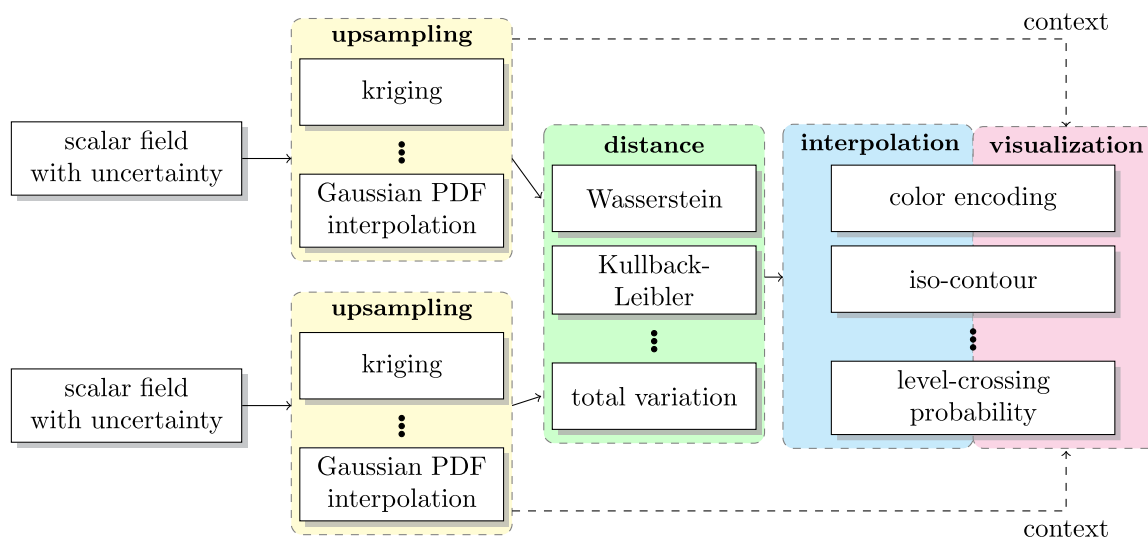


Fig. 1 Overview of the framework, which illustrates the major stages: *upsampling*, *distance*, and *interpolation/visualization*. Each of the two random fields is passed to one of the upsampling methods, which is followed by a distance calculation processing both upsampling results, and an illustration of the distance through a visualization method, which

might employ an additional interpolation. The dashed arrows indicate that visualizations in the explicit encoding paradigm need additional context from the upsampled scalar fields with uncertainty to help interpreting the presented distances

layout the underlying data is not present which results in a decontextualization, subsequently the interpretation of the observed difference is more challenging [54].

In the past, several authors worked on the issue of visually comparing scalar fields with uncertainty or ensembles in an explicit encoding. However, we identified a gap to directly visualize the difference of two or more scalar fields with uncertainty. The following related works are methods, which are most related to a direct comparison and visualization in an explicit encoding. Köthur et al. [26] extended the windowed cross-correlation matrix to time-varying ensembles to visualize the statistical properties of each cell as a glyph. Obermaier et al. [36] used volume rendering to encode different properties to present similarities or disagreements of time-varying ensemble trends. Therefore, they identified and tracked trends through time to present the statistical properties compared to the whole ensemble. Shu et al. [52] defined behavior vectors to identify similar clusters. Given a target location, a behavior vector is the collection of differences of all ensembles at this location. These multi-dimensional vectors form clusters in neighboring regions, which are visualized in a dense overview visualization. Rubner et al. [46] introduced the *earth mover's distance* and used multi-dimensional scaling to explore image databases. In addition, this allowed to search an image database based on color-distribution and texture spaces.

The framework we present is built on three actively researched, major research areas in the context of visual comparison: interpolation of scalar fields with uncertainty, distance of random variables, and visualization of (uncertain) scalar fields. All the existing methods of those research

areas can be used in our proposed framework. One of the most used methods to compare scalar fields with uncertainty is to illustrate them in a juxtaposition using contouring or volume rendering techniques. Pöthkow et al. [40, 42] proposed ways to present the positional uncertainty of iso-contours. In addition, Pfaffelmoser et al. [39] presented an incremental update scheme in the volume ray-casting, which considers the uncertain data. Further improvement in the iso-contour/iso-surface of uncertain data is done by Athawale et al. [1–3]. Another work in presenting uncertain three-dimensional data was presented by Djurcilov et al. [11] through mapping the mean values to color and uncertainties to opacity. This allows to adjust the volume rendering to show uncertain areas more opaque, while illustrating values with high certainty. The reader is referred to the present surveys for an in-depth summary about uncertainty visualization [6, 7, 21, 38].

The research on interpolating scalar fields with uncertainty is spread over different communities and fields, namely mathematics, geographic information systems, and visualization. For now, we only focus on the interpolation methods introduced to the visualization community, as even a brief overview of all methods would be beyond the scope of this article. Pöthkow et al. [40] explain an interpolation method, the *Gaussian probability density function (PDF) interpolation*, which interpolates the moments (mean and standard deviation) of Gaussian distributions in their work. Sakhaee et al. [47] took a different approach and identified the close relation of box splines to the weighted linear combination of random variables in their volume rendering algorithm. The interpolation method *kriging* was introduced into the context we discuss by Schlegel et al. [49]. *Kriging* is a Gaussian

process regression of a set of random variables at arbitrary positions. Besides the definition of Schlegel, there exist many variations in *kriging* [30]. Hollister et al. [17] introduced two interpolation methods, namely *gaussian mixture model (GMM) PDF interpolation* and *quantile PDF interpolation*. The first one interpolates the parameters of a Gaussian mixture model, while the *quantile PDF interpolation* interpolates the probabilities of the quantiles of the PDFs. Further interpolation methods can be found in the work of Myers [35], and Li and Heap [30].

Distance metrics on random variables are not new to the visualization community, as some authors used statistical distance functions to illustrate errors, differences, or convergence criteria to assist their argumentation. Rubner et al. [46] used the *earth mover's distance* (Wasserstein distance) as a measure when calculating the distance of color distributions and textures. In addition, Siddiqui et al. [53] used the same measure to present the convergence of their progressive approach in diffusion tensor imaging by calculating the distance of histograms, while Hoand et al. [16] tested different metrics to calculate the error of histograms in their analysis of the trade-off between reducing image precision or resolution. In contrast with our proposed framework to compare a whole scalar field with uncertainty, the aforementioned publications only process two random variables, e. g., two distributions [46] or histograms [16, 53]. However, as far as we are aware, there is not a published work in the literature that discusses the comprehensive application of distance functions on an entire scalar field with uncertainty.

Cha [9] presents a survey on statistical distance or similarity measured on random variables. In addition, Grigorenko et al. [14] recently presented two methods to construct probabilistic distance functions from statistical distance metrics. Please note, probabilistic distance functions can be characterized by probabilistic metric spaces [51], which are initially introduced as statistical distance spaces [33], which should not be confused with the statistical distance functions summarized by Cha and further used as fuzzy metrics [27]. We opt to term this class of functions *probabilistic distance functions* to emphasize their distance of probabilistic nature.

3 A framework for visual comparison of scalar fields with uncertainty

Designs in explicit encoding show relationships between objects explicitly in a single visualization [13]. This requires the knowledge of the relationships of interest and a way to compute them explicitly. For scalar fields with uncertainty, the objects of interest are the random variables on the grid points and the relationship of interest is the dissimilarity between them.

Figure 1 shows an overview of the introduced framework, which processes two scalar fields with uncertainty through a three-stage pipeline to create a comparative visualization in explicit encoding. The three stages—*upsampling*, *distance*, and *interpolation/visualization*—classify and organize the necessary techniques to create dense representations of differences. Depending on the distance function utilized in the *distance* stage, the resulting visualizations can convey various meanings, such as (dis)similarities or average mutual information [29]. The benefit of dense visualizations in explicit encoding design is the direct identification of differences that result in a fast location of areas of interest. In order to be able to properly interpret the dense visualization in the explicit encoding, the resultant visualization should contain a context from one or both inputted scalar fields with uncertainty.

The *distance* stage is the core of this framework allowing to encode a desired relationship into a scalar field with or without uncertainty, which then can be visualized by the *interpolation/visualization* stage. The *interpolation/visualization* stage is a twin stage because many of visualization techniques for scalar fields highly depend on interpolation, e. g., volume rendering and marching cubes. In the comparison of scalar fields with uncertainty, interpolation of the distance can lead to misleading visualizations. Figure 2 shows a simple one-dimensional example of interpolating two random variables before (right column) and after (left column) distance calculation. In these two scenarios, the final visualization (bottom row) differs. To address this challenge, our framework starts with an *upsampling* stage that involves interpolating the scalar fields with uncertainty prior to computing the distance of the desired relationship. To avoid confusing the term interpolation of the *interpolation/visualization* stage with the interpolation of the *upsampling* stage, we use the term *upsampling* if we write about the *upsampling* stage and use the term *interpolation* otherwise.

The three stages of our framework fit well into the steps commonly considered to be constituent parts of the overall visualization process, that is, the so-called visualization pipeline [55, p. 124][18]. Thus, the framework can be easily used in the context of existing visualization systems or approaches. Specifically, the *upsampling* and *distance* stages can be seen to belong to the *filtering* part of the pipeline, whereas the *interpolation/visualization* stage goes with the *mapping* part.

The subsections of this section provide an in-depth exposition of each stage and offer an examination of the underlying processes. Of particular note is the grouping of methods within each stage, predicated on shared characteristics that wield substantial influence over the resulting visualization. The systematic categorization of these methods based on commonalities not only facilitates a more profound under-

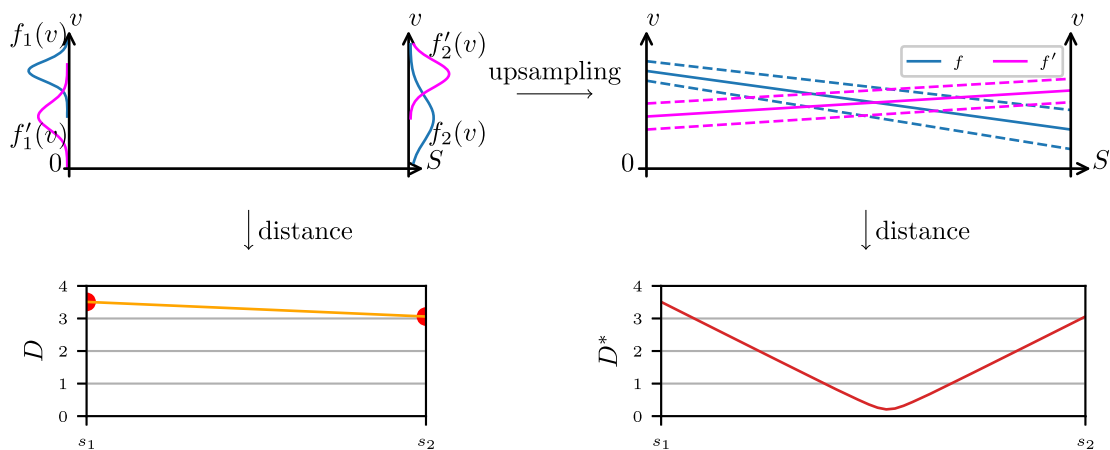


Fig. 2 Left column illustrates the distance D (bottom) as red points of the two distributions f and f' at the positions s_1, s_2 (top). The orange line in the bottom plot indicates the interpolation of the distances D . The right column (top) illustrates an upsampling of the same distribu-

tions f, f' , while the continuous lines indicate the mean and the dashed lines indicate the standard deviation. The bottom of the right column presents the distance D^* of the interpolated uncertain distributions

standing but also reveals essential patterns that govern visualization. Section 4 concludes the description of this framework by summarizing the existing interdependencies between methods spanning different stages.

3.1 Scalar fields with uncertainty

Scalar fields with uncertainty are defined as grids with random variables on their nodes. Random variables can be modeled through a PDF, by a histogram, or as a Gaussian distribution to name a few commonly known possibilities. Let S be a subset of \mathbb{R}^2 or \mathbb{R}^3 that contains a finite number of positions $s_i, \dots, s_N \in S$. At each position, a random variable X_1, \dots, X_N defines the grid attributes. For simplicity, we omit the covariance between each random variable and leave its inclusion to future work. Furthermore, let two scalar fields with uncertainty $\mathbf{X} = \{X_1, \dots, X_N\}, \mathbf{Y} = \{Y_1, \dots, Y_N\}$ be defined at the same positions $s_1, \dots, s_N \in S$. The modeling of the two scalar fields with uncertainty is of minor interest because the random variables on the grid points can be converted to different representations. For example, the moments of a Gaussian distribution (mean, variance) can be used to create histograms or PDFs. The desired representation of random variables is primarily dependent on the upsampling method. Some upsampling methods are restricted to Gaussian distributions or histograms.

3.2 Upsampling stage

Upsampling, a fundamental concept in signal processing and data analysis, involves the approximation of a continuous function based on a given set of discrete samples. It aims to create an approximation that emulates what the continuous function would have been had it been sampled at a higher rate.

The upsampling process is characterized by a universal rate increase factor denoted by L , which is typically an integer that determines the desired target sampling rate.

All the upsampling methods that can be embedded in the *upsampling* stage return a scalar field with uncertainty. Hollister et al. [17] formulated three criteria that an upsampling method should fulfill for scalar fields with uncertainty: (i) the upsampled PDFs should not introduce additional modes, (ii) the lower limit of the upsampled variance should have a smaller variance at the observed grid points, and (iii) the upsampled values should be PDFs. In addition, Schlegel et al. [49] argued that (iv) the variance between the grid points should increase as information of the unknown distributions toward the center accumulates to a more uncertain mean value. Unfortunately, the literature lacks definitions of constraints on the properties that the covariance should follow for the upsampling process, but this lack does not restrict this framework to the usage of upsampling methods considering the covariance. These restrictions must follow the target application. For the interested reader, Sect. A in appendix shows three exemplary upsampling methods, which satisfy different criteria.

Following the statement of Pöthkow et al. [41], we advise in modeling uncertain scalar fields with nonparametric models and upsample them with the supporting methods to aim for an optimal fit. However, only a few upsampling methods allow upsampling of non-Gaussian distributions. Section 4 gives an overview of a few upsampling methods and which representations they support.

3.3 Distance stage

A distance is a quantitative measure that relates to two points, which in our context are random variables. Intu-

itively, when we consider the distance between two points in a two-dimensional plane, we often conceptualize it as a representation of the spatial gap that separates them. However, when the two-dimensional plane corresponds to a feature space, this interpretation changes into an assessment of how dissimilar these points are in terms of their characteristics. The application of statistical distance functions extends this concept to random variables, offering a means of gauging the dissimilarity between them. In this way, distance functions become invaluable tools for summarizing the disparities between the corresponding points within two scalar fields with uncertainty, providing a holistic overview of areas of interest and aiding in the quantitative assessment of data relationships.

Distance functions can be characterized and classified based on four axioms of a metric. Depending on the accomplishment of the four axioms, a distance function offers varying properties, whereas it is only called a metric if all four axioms are satisfied. Formally, a distance function $d : M \times M \rightarrow \mathbb{R}$ is a metric on the set M if it satisfies the following axioms for all points $x, y, z \in M$ [8]:

(d1) (Identity) The distance from a point to itself is zero:

$$d(x, x) = 0$$

(d2) (Positivity) The distance between two distinct points is always positive:

$$d(x, y) > 0, \text{ if } x \neq y$$

(d3) (Symmetry) The distance from x to y is equal to the opposite direction y to x :

$$d(x, y) = d(y, x)$$

(d4) The triangle inequality or subadditivity holds:

$$d(x, z) \leq d(x, y) + d(y, z)$$

Back in our context of distance functions on random variables, many prominent similarity measures are not a metric. For example, the Kullback–Leibler [9] divergence D_{KL} is a divergence that satisfies only the identity (d1) and positivity (d2) of the metric axioms. Thus, using the Kullback–Leibler divergence D_{KL} in our framework, the user should be aware that the symmetry axiom (d3) is not satisfied. This results in points $X_i \in \mathbf{X}, Y_i \in \mathbf{Y}$ not having the same distance $D_{KL}(X_i, Y_i) \neq D_{KL}(X_j, Y_j)$ even though the distributions are equal $X_i = Y_j, Y_i = X_j$ but at a different point $s_i \neq s_j$. In other words, the resulting visualization encodes different values for the two locations, while their distributions are simply switched. This can lead to misinterpretation, e. g.,

assuming that the distances of both locations differ. However, the Kullback–Leibler divergence is widely used in the context of machine learning [29]. Thus, we do not limit our framework to metrics, but rather motivate researcher to be aware which axioms a distance function satisfies.

This framework is built to support two classes of distance functions: statistical distance functions, and probabilistic distance functions. These two classes of functions describe the dissimilarity between random variables in different ways. Statistical distance functions summarize the distance between two random variables in a scalar value. In contrast, probabilistic distance functions provide a distribution of the difference. It should be noted that this article distinguishes between the term *difference*, which for random variables results in a distribution (e. g., a PDF of the difference), and the term *distance*, which is a scalar value. Analogous to scalar values, the difference between two values can be converted into a distance, e.g., by taking the absolute value of the difference. This conversion is not that simple for random variables and thus is done using statistical distance functions.

The axioms of a metric are still applicable for statistical distance functions because they map two random variables to a scalar value. However, probabilistic distance functions return distributions, and thus, the aforementioned axioms are no longer applicable. Probabilistic distance functions can be similarly classified based on a distribution function $F_{pq}(x)$ using four axioms [51] with the same names. Here, the distribution function $F_{pq}(x)$ acting on the random variables p and q with $x \in \mathbb{R}$ being a real argument is a probabilistic distance metric if it satisfies the following conditions [33, 50, 51]:

(D1) (Identity) The distribution function equals one for all x only if both random variables are equal:

$$F_{pq}(x) = 1, \text{ for all } x > 0 \text{ if, and only if, } p = q$$

(D2) (Positivity) The distribution function has only positive values:

$$F_{pq}(x) = 0, \text{ for all } x \leq 0$$

(D3) (Symmetry) The difference between p and q is equal to q and p :

$$F_{pq}(x) = F_{qp}(x)$$

(D4) The triangle inequality or subadditivity holds using a 2-place function T :

$$F_{pq}(x + y) \geq T(F_{pq}(x), F_{pq}(y)), \text{ for all } x, y \geq 0$$

The conditions on the distribution function $F_{pq}(x)$ have similar affects on the resulting visualization like the statistical distance functions. Thus, researchers must be cautious about the properties of a distance function.

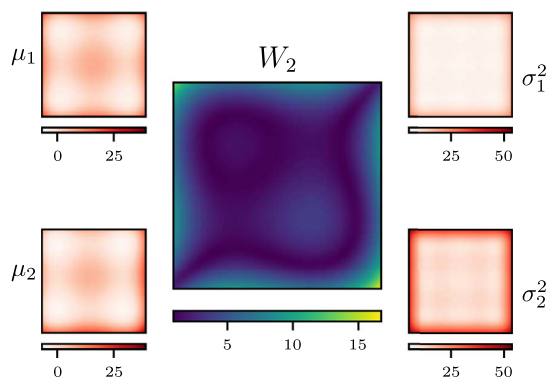


Fig. 3 Difference (Wasserstein distance W_2 in the center) between two data sets $\mathbf{A} \sim \mathcal{N}(\mu_1, \sigma_1^2)$ and $\mathbf{B} \sim \mathcal{N}(\mu_2, \sigma_2^2)$ is difficult to interpret, even if both data sets with uncertainty (means μ and variances σ^2) are present in the corners of the visualization. The second data set \mathbf{B} differs in its mean μ_2 by a positional offset and the variance σ_2^2 is doubled, compared to the first data set \mathbf{A}

3.4 Interpolation/visualization stage

In the final stage, *interpolation/visualization*, two different types of inputs must be considered. While scalar values can be investigated using visualization methods for scalar values, probabilistic differences must be illustrated using appropriate visualization techniques with uncertainty in mind. Illustrating the differences represented by density distributions is a challenging task. Fortunately, these density distributions can be interpreted as scalar fields with uncertainties. However, the literature lacks methods that consider these density distributions. Further research is needed to investigate the known methods that can be used to create expressive visualizations. As a first step, we present the *differences* using a basic uncertainty visualization technique, such as the LCP [40, 42].

Besides visualizing solely the distances, the visualization should consider the context of at least one data set. The motivation behind this is the work of LYi et al. [32], which summarizes the weaknesses of the explicit encoding paradigm. A major problem in solely visualizing differences as an explicit encoding is decontextualization. This occurs if only one specific relationship without the original information is presented and the viewer is missing the context of the original data, as shown in the visualization in the center of Fig. 3. This visualization shows the point-wise Wasserstein distance W_2 between the two scalar fields with uncertainty. The differences can be identified quickly, but their interpretation becomes infeasible without considering the differences in relation to the original data, as shown in the corners of Fig. 3.

3.5 Visualization of context

To avoid decontextualization, researchers tend to use hybrid approaches such as simply juxtaposing the difference and the original data. A more complex approach to overcome this weakness is to superimpose at least some details of one of the original data sets into the visualization of the distance. This is particularly challenging for complex data, such as scalar fields with uncertainty. Please note that this framework does not provide a general approach for dealing with decontextualization, but is motivated by the dashed arrows in Fig. 1 to consider this issue. We want to share how we deal with decontextualization of the comparison of scalar fields with uncertainty.

Following the suggestions of LYi et al. [32] to use hybrid layouts, such as juxtaposing or superimposing the distance and the original data sets, which showed superior performance compared to a single layout, we focused on superimposing the original data on the explicitly encoded comparison. However, this framework is not limited to this approach as it includes the context into a visualization that can result in multiple linked views. A comparison always deals with at least two data sets, which opens the following question: Is it sufficient to only visualize one data set or is it necessary to present both data sets to include the context of both in the comparative visualization?

Presenting all, the difference and a context of both data sets in one visualization are a challenging task if occlusions should be minimized. This is especially difficult for complex data with uncertainty, because each data point represents an entire distribution of values. Embedding of a characteristic feature may be helpful in reducing the amount of information. Fortunately, the literature offers a wide range of methods for visualizing features of scalar fields with uncertainty, e. g., [20, 42, 48, 56]. This approach is applied in Fig. 4 visualizing the difference between both data sets as contours, while the LCP [40] of both data sets is superposed into the explicit encoded visualization. Based on a two-dimensional approach, we identified an approach for three-dimensional data. This involves visualizing the intersection of the super-level set of LCPs alongside the volume rendering of the differences (see Fig. 6). This approach has the handy effect that an absence of the intersection indicates a difference between the original data sets and thus leaves space to visualize the difference that occurs at this location.

4 Framework instances

We now aim to provide constraints on how to build instances of our proposed framework. The main purpose of this framework is to create comparative visualizations of scalar fields with uncertainty. These visualizations contain information about the extent to which random variables differ at each point. A desired property of the visualization is that all statistical properties are considered in the comparison.

The methods used in the *upsampling* stage are highly dependent on the data that they support. Table 1 provides an overview of the mentioned upsampling methods and their applicability for upsampling scalar fields with uncertainty based on their representation. Versatile upsampling methods, e. g., ensemble PDF interpolation [49], can be applied to all representations, but these methods have drawbacks in terms of their runtime or precision. Please note that not all upsampling methods consider covariance.

The choice of a distance function used in the *distance* stage is twofold based on the decision of the researcher to inspect the difference/distance (statistical distance or probabilistic distance) and which aspect of the dissimilarity of two scalar fields with uncertainty are of interest. The latter is purely motivated by the knowledge a scientist wants to gain. There exist no constraints of distance functions on the used upsampling method or on how the scalar fields with uncertainty are represented. However, certain representations of the uncertain scalar field offer benefits by allowing a distance function to compute the distance efficiently using a closed form. This aspect will be elaborated upon in subsequent sections of this article.

Finally, the visualization methods of the *interpolation/visualization* stage must be able to visualize either scalar fields representing the *distance* or scalar fields with uncertainty representing the *difference*. For scalar data types, the literature offers many of visualization methods for exploring the dissimilarity of the input data. This is not the case for scalar fields with uncertainty representing *differences* as these distributions have never been introduced to the visualization community. Thus, further research needs to be conducted on how and if the available methods are able to properly visualize the *differences*.

An exemplary instance of this framework is as follows: Two scalar fields with uncertainty represented as Gaussian distributions are both upsampled using *Gaussian PDF interpolation* [40] and the point-wise Wasserstein (Earth Mover's) distance [22] between the interpolated uncertain fields is then visualized using direct volume rendering (DVR). The resulting visualization now contains information ranging from $[0, \infty) \in \mathbb{R}$, representing how much the random variables at each point differ. A value of zero occurs only if both random variables at the same position are equal. The more the

random variables differ in their distribution, the higher the distance between them.

5 Experiments

In our experiments, we showcase the versatility of our framework through comparative visualizations across diverse data sets from various domains, each with its unique research question. A prominent synthetic data set to begin with is the tangle function [25] enhanced with uncertainty to introduce how the difference in the mean and/or variance affects the visualization, followed by an experiment in the research area of climate simulation [37] to determine how the forecasts of the two simulation models differ. Moreover, we illustrate the use of this framework within a medical context [44] using the blood oxygen level dependent BOLD time series to explore altered brain activity in patients with schizophrenia. In this context, we performed two experiments: identifying areas of interest between two subjects and finding subject pairs that differed the most. Finally, we investigated the climate simulations [37] again, but now we use a probabilistic distance function to explore the *difference* between the two models. This basic method is the first step toward closing the gap in the literature by visualizing the *difference* between two scalar fields with uncertainty represented by a distribution function.

In addition to presenting how the framework can be used to create comparative visualizations, we used the framework as a guideline to talk about creating comparative visualizations. After a short introduction to each experiment, we elaborate on how each stage of the framework was used to explain the resulting visualization. This structured approach, similar to the visualization pipeline, helped us elucidate the presented visualizations.

We implemented this framework using OpenWalnut [12], which is an open-source project. The non-optimized implemented methods were published in the project as modules. Visualizations were created using *ParaView* [4]. The experiments were executed on a system with an Intel Core i7 6700K, 50 GByte RAM, and an NVIDIA GeForce GTX 1080.

5.1 Synthetic: tangle function

The purpose of this experiment is to provide the reader a first intuition on how various properties of the comparison of random variables influence the visualization. Assuming Gaussian distributions, two random variables can differ in their mean and/or variance. We prepared four data sets that differ in the ways a Gaussian distribution can differ (see Fig. 4): b) only the mean differs, c) only the variance differs, d) both mean and variance differ, and a) no difference at all. We used the first quadrant of the two-dimensional slice of the tangle function [25] as our area of interest. We modeled

Table 1 A tabulation of upsampling techniques and their applicability for upsampling scalar fields with uncertainty represented by Gaussian distributions, GMM, and nonparametric PDFs

Gaussian PDF interpolation [40]	✓		
Kriging [49]	✓		
GMM PDF interpolation [17]	✓	✓	
Quantile PDF interpolation [17]	✓	✓	✓
Box-spline interpolation [47]	✓	✓	✓
Ensemble PDF interpolation [49]	✓	✓	✓
	Gaussian distribution	GMM	nonparametric PDF

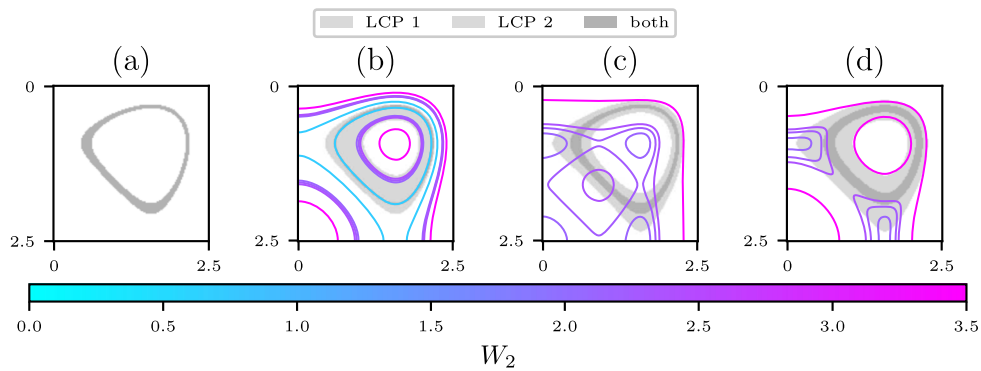


Fig. 4 Comparison of variants of the first quadrant of the tangle function. In the images **a–d**, the variants **a** do not differ, **b** differs only regarding the mean values, **c** differs only regarding the variance, and **d** differs regarding the mean and the variance. The contour lines represent

the difference W_2 while the shades of gray represent the superlevel set ($\geq 45\%$) of the LCP of both original data sets. Visualizing the LCP provides context for the visualization of the difference

different scenarios in which a Gaussian distribution may vary using this area of interest.

Following the framework, we use an upsampling factor of 2 for the *Gaussian PDF interpolation* [40], which fulfills criteria (i)–(iii) of Holister et al. [17], but does not satisfy criterion (iv) of Schlegel et al. [49]. It is not necessary to fulfill the last criterion of Schlegel et al., because the tangle function is a smooth function, which we sampled sufficiently high to assume a linear change between the grid points. We aim for a visualization that provides insights exclusively when there are differences between random variables at a grid point, thereby adhering to the condition outlined in identity (d1). In addition, the distance should be symmetric (d3) so that the reader can identify areas of equal dissimilarity. Finally, we present the four cases in separate visualizations; thus, we require the triangle inequality (d4) to hold in order to be able to compare the four cases. The *Wasserstein* metric W_2 satisfies all the properties (d1–d4) required for a metric, making it suitable for this particular task.

Figure 4 shows the difference between the four cases as color-encoded contour lines, while the superlevel set ($\geq 45\%$) of the LCP [40] includes both original data sets to add a context. As this visualization already contains a lot of information, both LCP have the same gray color, as only their intersection is of major interest. For the case of no difference, Fig. 4a visualizes zero distance and fully overlapped

LCPs. In the second case in Fig. 4b, the mean values differ; thus, the LCP does not overlap. Because we know that only the mean values differ, the Wasserstein distance W_2 is equal to the absolute difference between the mean values. In Fig. 4c, only the variance differs, which is equal to the absolute difference in the standard deviation. The LCPs of both original data sets have maxima at the same locations; however, owing to different variances, the possible location of one LCP is wider. Both the mean and variance differ in Fig. 4d which results in the highest distance in the center of the visualization. Here, it is not possible to identify the influence of the mean or variance on distance. However, we can identify that the distance is higher than in the other cases, which serves as an entry point for further investigation. The LCPs now overlap similar to the third case in Fig. 4c; however, based on different mean/variance, their maximal estimated location and width differ.

The presented visualizations allow us to quickly identify dissimilarities between the data sets and provide an overview for further investigations. To give an example considering only Fig. 4d, the reader can quickly identify the local maxima in the center of the visualization (1.7, 1.0) which decreases toward the bottom and left of the visualization. In addition, the differences increase toward the bottom-left corner (0, 2.5) and upper/right of the visualization.

5.2 Climate simulation: DEMETER

In this experiment, we want to exemplify how a researcher for climate simulations can use the proposed framework to compare two simulation models based on their forecasts. For example, the DEMETER project [37] used seven climate models, each producing nine different forecasts. Ensembles of climate simulations can be interpreted as samples of one scalar field with uncertainty. First, we use two models that forecast the temperature for the February 20th in the year 2000 and want to know for which regions the forecasts of both models differ.

The ensemble is sampled only by 20 points both in longitude and latitude and 3 for the height; thus, we cannot assume a linear change in temperature; in other words, we are unsure about the temperatures between grid points. The upsampling method *kriging* [49] allows us to model this uncertainty between the grid points, which satisfies all upsampling criteria (i)–(iv). We used an upsampling factor of four to effectively consider the increased uncertainty between the grid points. The *Kullback–Leibler* [9] divergence $D_{KL}(X_i, Y_i)$ is a well-known distance function in the context of machine learning, which we want to use here. Given two models \mathbf{X}, \mathbf{Y} of the DEMETER project, represented as two scalar fields with uncertainty using Gaussian distributions, we compute the point-wise distance $D_{KL}(X_i, Y_i), X_i \in \mathbf{X}, Y_i \in \mathbf{Y}$. This distance function is a divergence that satisfies only the identity (d1) and positivity (d2) of the metric properties. Therefore, even if the areas exhibit similar values in the resulting visualization, this does not imply that they have similar differences. However, for this task it is not necessary to satisfy the triangle inequality (d4) because we do not want to compare the differences of the points or more than two models. Finally, we visualized the differences between the forecasts of both models using direct volume rendering.

Figure 5 shows the direct volume rendering of the Kullback–Leibler divergence. To compensate for the decontextualization, we included the intersection of the superlevel sets ($\geq 45\%$) of the LCPs of both original data sets. Note that the absence of the intersection of the LCPs indicates a difference between the two forecasts. This absence mostly occurs close to the equator and can be identified directly by the Kullback–Leibler divergence. Note that the intersection surface is not smooth owing to the increased LCP between the grid points, which has an increased uncertainty due to the upsampling method. This visualization provides a good entry point for further investigation of the region of interest.

5.3 Medical data set

In this experiment, we want to identify areas of interest for a further analysis of the functional connectivity of schizophrenia. This [OpenNeuro Dataset ds000115](#) [44] consists of

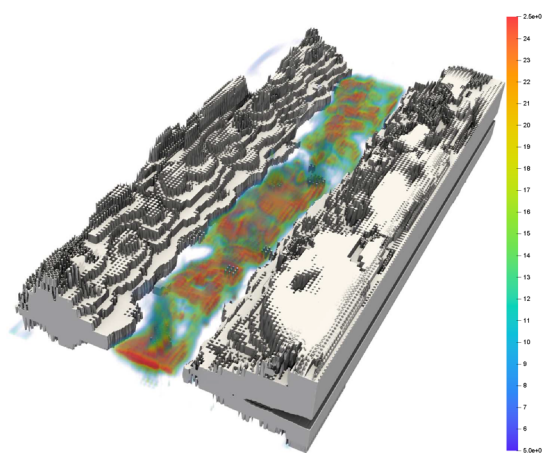


Fig. 5 Volume rendering of the Kullback–Leibler divergence between the forecasts of two models. In addition, the shown iso-surface is the intersection of the superlevel sets ($\geq 45\%$) of the LCP at -63.15°C of both original data sets

measurements of BOLD time series of 99 individuals with schizophrenia, their unaffected siblings, a healthy control group, and their siblings. During the scan, the subjects performed a task to increase their working memory load. Repovs et al. [45] analyzed the difference in the working memory loads of the brain connectivity of several areas. In our experiment, we want to compare the entire measured data of one subject to one or more subjects. For this, we summarized each normalized time series of a measurement as a scalar field with uncertainty using a Gaussian distribution and then registered the mean scalar fields to a common base. Thus, the mean can be interpreted as the resting state, while the variance increases with a higher working memory load.

The resolution of this data set after we converted it into a scalar field with uncertainty is $64 \times 64 \times 26$ which we want to increase by an upsampling factor of 2. We assume this data set is sampled highly enough to use the *Gaussian PDF interpolation*. Symmetry (d3) and identity (d1) are the properties we need for the distance function to identify the locations of interest. In addition, it would be handy to be able to compare several subjects to one base subject to judge how the comparisons differ. Thus, the desired distance function should satisfy the triangle inequality (d4). For this, we can employ the point-wise *Wasserstein* distance W_2 , which is a metric satisfying (d1)–(d4).

Figure 6 shows, similar to our synthetic data set, the intersection of the superlevel set ($\geq 45\%$) of the LCPs of both data sets as a context to present the Wasserstein distance as a volume rendering. Please note, to avoid visual clutter, the visualization includes only one half of the brain. This helps to identify that the presence of a high difference coincides with the absence of the intersected LCPs. In this visualization, the areas of interest can be identified by the presence of a difference, which can be quickly identified through the

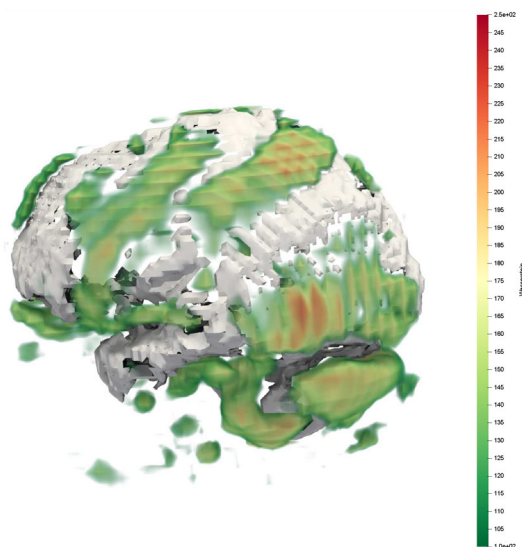


Fig. 6 Volume rendering of the comparison (Wasserstein distance) of summarized BOLD signals of two subjects with and without schizophrenia. As context, an iso-surface (intersection of LCP super-level set for 45%) of both subjects is rendered

visualization. High values indicate that both subjects had a different cognitive load in those areas and further investigations inspecting the functional connectivity of those areas could be made.

A follow-up question is which participants differ the most/least to further inspect a reason behind those differences. This task involves the comparison of several uncertain scalar fields with uncertainty. Opting for the Wasserstein distance W_2 proves advantageous as it adheres to the triangle inequality (d4), enabling us to make estimations between comparisons. While this experiment did not result in a volumetric visualization, like the previous one. It is an example of how this framework can be used to make or think about more abstract comparisons of scalar fields with uncertainty.

In the previous experiment, we computed the point-wise distance using the Wasserstein metric W_2 . Now, we consider the whole three-dimensional image as a multivariate distribution without covariance. At this point, we do not want to upsample individuals (upsampling factor $L = 1$), so we do not apply any upsampling method. Similar to the visualization pipeline, this is still valid in our proposed framework. For the *distance* stage, we use the Wasserstein metric W_2 for multivariate distributions, which results in a single scalar value of how much both images differ. This allows us to create a distance matrix between individuals. We then visualize this distance matrix as a heat map to identify which subjects differ the most/least.

Figure 7 shows the normalized distance matrix between each subject pair in a heat map. We grouped the individuals based on their condition: individuals with schizophrenia

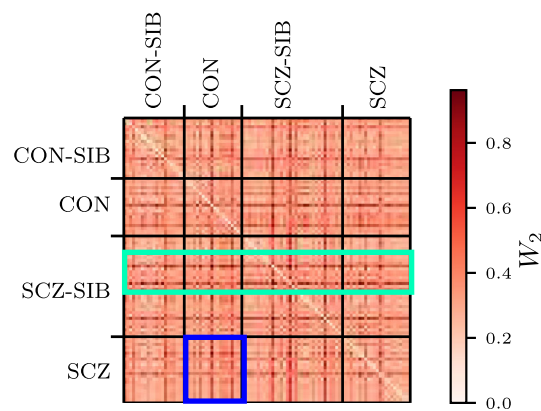


Fig. 7 Heat map of the normalized distance matrix of all subject pairs utilizing the Wasserstein distance W_2 . The comparison of individuals with and without schizophrenia is highlighted with a blue rectangle. The turquoise rectangle highlights individuals without schizophrenia to also have a high difference to all other individuals

(SCZ), their unaffected siblings (SCZ-SIB), a healthy control group (CON), and their siblings (CON-SIB). Within the groups, the individuals are sorted by age. This visualization allows the reader to quickly get an overview of the whole data set. We observe that the comparison between individuals with and without schizophrenia, indicated by a blue rectangle, encompasses subjects exhibiting both high and low dissimilarity. However, we can find a pair of individuals having a very high dissimilarity in their brain activity which could be investigated further. In addition, we can identify that some siblings of individuals with schizophrenia, marked in the turquoise rectangle, have a high dissimilarity to all other individuals. From this point of view, additional methods, e.g., clustering methods, can be applied to further investigate this data set. However, this is not the scope of this article.

5.4 Probabilistic distance

This experiment introduces a new type of comparative visualization that employs probabilistic distance functions to create a scalar field with uncertainty, encoding how much two scalar fields with uncertainty *differ*. For this purpose, we used the two models \mathbf{X} , \mathbf{Y} from the DEMETER data set of the previous experiment. Please note, we are interested in the *difference* (a distribution) and not the *distance* (a scalar).

We want to focus solely on the probabilistic distance function; thus, we do not apply an upsampling method. A novel article by Grigorenko et al. [14] describes two methods to create probabilistic metrics based on statistical distance functions. We use the probabilistic metric *standard GV-fuzzy metric* $F_{pq}(x)$ with the total variation distance $\delta(p, q)$ as described by Grigorenko et al.:

$$F_{pq}(x) = \frac{x}{x + \delta(p, q)} \tag{1}$$

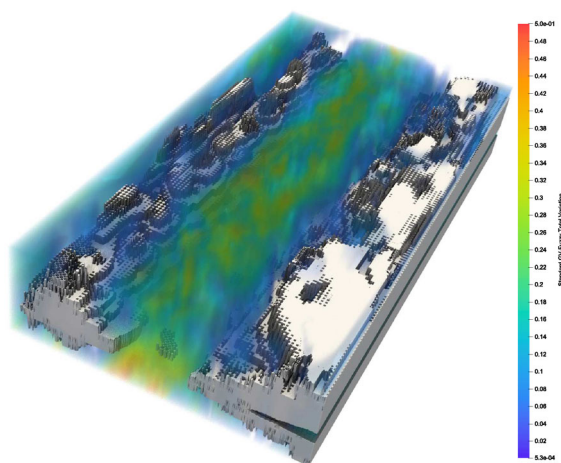


Fig. 8 Direct volume rendering of the LCP showing the most occurring differences ($LCP_{60}(\mathbf{F})$). Please note the *difference* \mathbf{F} is represented as a scalar field with uncertainty which can only be visualized using uncertainty visualization methods. The white surface is the intersection of the superlevel set ($\geq 45\%$) of the LCPs of both original data sets at a temperature of -63.15°C

$$\delta(p, q) = \frac{1}{2} \sum_t |p(t) - q(t)|, \quad (2)$$

while p, q are the PDFs for each pair of points $X_i \in \mathbf{X}, Y_i \in \mathbf{Y}$. This probabilistic metric fulfills all properties of a metric (D1)-(D4). In order to visualize these differences $\mathbf{F} = \{F_{pq}(x), \forall p \in \mathbf{X}, \forall q \in \mathbf{Y}\}$ represented as distributions, we need to use an uncertainty visualization method. We opt for the use of the LCP [41] to have an initial view of this scalar field with uncertainty. Please note the random variables $F_i \in \mathbf{F}$ at the grid points i are no Gaussian distributions and their values are strictly positive because the distance function satisfies the positivity (D2). We will further denote $LCP_x(\mathbf{F})$ for the LCP at the value x of the *difference* \mathbf{F} . This uncertainty visualization method may not be the best choice, but identifying a well-suited method is beyond the scope of this article and is kept for future work.

Figure 8 shows the direct volume rendering of the LCP adjusted to show the most occurring differences for the value of 60, denoted as $LCP_{60}(\mathbf{F})$. In other words, the visualization shows the feature probability of a specific *difference* \mathbf{F} between both models. In addition, the visualization includes the intersection of the superlevel set ($\geq 45\%$) of the LCPs for the temperature -63.15°C . The result supports the findings of the previous experiment using the statistical distance function. The areas where both models produce different results are close to the equator. This visualization contains more information about the *difference* than the previous experiment using a statistical distance function (see Fig. 5). However, this visualization only shows one feature probability $LCP_{60}(\mathbf{F})$ of the whole difference. Thus, the probabilistic distance \mathbf{F} contains more information than the aforemen-

tioned experiment. For the interested reader, we include additional visualizations of other values, e. g. $LCP_5(\mathbf{F})$, in appendix B.

6 Best practice guide

In this section, we present a more general approach to creating visualizations using the proposed framework. Choosing the correct method for the *upsampling* stage initially depends on how the uncertainty in the present data sets is modeled. In most cases, owing to the central limit theorem, scalar fields with uncertainty are modeled to contain Gaussian distributions at their vertices. Based on Table 1, all listed methods support the interpolation of Gaussian distributions. Now, one open question remains: "Which upsampling criterion mentioned in Sect. 3.2 should be fulfilled?" While the answer to this question follows the target application, a straightforward approach is to choose Gaussian PDF interpolation [40]. This method assumes that a scalar field with uncertainty is sampled sufficiently enough to ensure only linear changes in the interpolated values. Owing to its linearity, artifacts in the resultant visualization are minimized and an upsampling factor of $L = 2$ is sufficient to avoid misleading visualizations, as shown in Fig. 2.

To identify a suitable upsampling method, we now summarize what each criterion implies and how the resultant visualization is affected by it:

- (i) *No additional modes*: Additional modes between two distributions with only one mode are desirable in the context of volume rendering materials where one point might encode the occurrence of multiple materials, such as the boundary between two different types on either side [17]. This property is undesirable for a distribution that should transition, such as the temperature at two different locations. It has no side effects due to the *distance* stage on the resultant visualization, in contrast with criterion (ii).
- (ii) *Lower limit of the upsampled variance*: This criterion, if not fulfilled, allows the uncertainty between two points to be smaller than that at the points. This is not only counter-intuitive but also affects the resultant visualization through the *distance* stage. A reduced variance results in a reduced or increased difference, and thus, can result in visual artifact.
- (iii) *Upsampled values have to be PDFs*: While this criterion is desirable for further work with PDFs, most of the distance functions are defined to operate on CDFs that can be converted from and to PDFs. However, Hollister et al. [17] mentioned this criterion to ensure that this type of conversion is valid. This criterion has no side effects on the resultant visualization.

(iv) *Increased variance for upsampled points*: This criterion makes the model of the upsampled points more uncertain. While the motivation behind this approach is sound, an increased uncertainty between points, similar to criterion (ii), can result in visual artifacts due to the reduced/increased difference.

Choosing an appropriate distance function starts when deciding whether the user is interested in the *distance* or *difference*. Regardless of the decision, it is advisable to choose a distance function that satisfies all the metric axioms (see Sect. 3.3). Thus, the interpretation of the resultant visualization has no constraints and can be intuitively performed. However, an interpretation of the *difference* using feature-based visualization methods such as the LCP demands increased cognitive loads. Thus, based on the current limitations of visualizing the *difference* in scalar fields with uncertainty, we advise the use of statistical distance functions to create intuitive visualizations. A simple and intuitive statistical distance function that satisfies all metric axioms is the Wasserstein (Earth Mover's) distance [22].

The following list summarizes how each metric axiom (see Sect. 3.3) affects the resultant visualization:

- (d1/D1) *Identity*: This property ensures that the visualization can encode if two points are equal. Failure to satisfy this axiom does not allow the identification of equal points.
- (d2/D2) *Positivity*: This axiom ensures that all the differences can be interpreted as a measure of distance without a sense of direction, similar to the absolute difference defined for scalar values.
- (d3/D3) *Symmetry*: The symmetry axiom ensures that two points have the same value as other two other points, but are switched in their positions. Creating visualizations while not satisfying this axiom one is not able to tell if two locations have similar differences. However, if the relationship of interest is not the difference, for example, the relative entropy, fulfilling this axiom is not necessary.
- (d4/D4) *Triangle inequality*: The triangle inequality ensures that the resultant visualizations can be compared. If one is only interested in the difference between two data sets while using a single visualization, fulfilling this axiom is not critical. However, by comparing two comparative visualizations to reason about the encoded differences, this axiom must be satisfied.

Choosing appropriate visualization methods comes along with a minimization of cluttering as this framework suggests avoiding the decontextualization of the explicit encoding paradigm by using additional information from the original data sets. Thus, the visualization of the difference should

focus on the information of interest, e. g., only high differences. This approach ensures free space in the visualization scene for additional context information, which we advise to fill with the intersection of feature probabilities of the original data sets. The process of adjusting both the calculated differences and the context should be performed in an iterative manner to minimize occlusion. A good starting point is to create an initial visualization of the difference and identify a feature probability that supports the initial visualization of the difference. Feature probabilities, which support the presented difference, are equal or similar at locations with a low difference but vary at locations where the difference is high. This can be effectively visualized by the intersection of two feature probabilities that leave room in the visualization scene only if both features differ. For example, Fig. 5 shows that most of the high differences are close to the equator and the intersection of the superlevel set of the LCP for temperature -63.15°C does not overlap with the volume rendering. The next iterations alter between focusing on the presented difference, e. g., filtering out more differences, and further minimizing occlusions by adjusting the feature probabilities. The resulting visualization contains the desired information about the difference and context while minimizing occlusions.

7 Discussion and limitations

This theoretical framework presents itself as a blueprint for comparative visualizations in the explicit encoding of scalar fields with uncertainty. This facilitates a rapid identification of areas of interest, serving as an initial overview for subsequent exploration. In the presented experiments, the visualizations allow to quickly identify the differences of the data sets while considering their uncertainty. However, this can also be a limitation of its visualizations as they are subject to the limitations of comparative visualizations in the explicit encoding paradigm. LYi et al. [32] summarized these limitations and how various authors overcame them. While this article proposes a general approach to include a context in form of feature probabilities of the original data sets, this is only one way to overcome the issue of decontextualization. Further research to improve the proposed framework solving the summarized limitations of visualizations in the explicit encoding paradigm [32] can yield to a more holistic method to create comparative uncertainty visualizations in the explicit encoding paradigm.

Typically, the majority of distance functions possess a closed form applicable to Gaussian distributions, resulting in computational complexity that remains constant. Conversely, when dealing with non-Gaussian distributions, these distance functions rely on representations such as the PDF [9], directly employing samples of an unknown distribution or the CDF.

Thus, the time complexity of the distance calculation depends on how many samples are taken or on the resolution of the PDF/CDF.

The probabilistic distance functions are still an ongoing research topic, especially for the visualization community. Proper visualization methods need to be identified to create intuitive visualizations for the *difference* of two scalar fields with uncertainty. In our experiment, we used the LCP to show them. However, further research has to be done to capture all information of the *difference* through proper visualization methods. Promising candidates are direct volume rendering methods which are suited for non-Gaussian distributions. Please note characterizing the distance function $F_{pq}(x)$ by a mean or variance is not precise due to it not being symmetric like the Gaussian distribution. Thus, the work of Djurcilov et al. [11] cannot be applied without further adjustments. The same holds for other volume rendering techniques, e. g. [3, 39, 47], which requires further research.

However, in order to create interactive visualizations of the differences, further research has to be done in the modeling of the distribution function $F_{pq}(x)$, because processing a whole distribution is not feasible for huge data sets. In our experiment, we computed the distribution function $F_{pq}(x)$ for each point with respect to a desired iso-value for the LCP. However, further research on how to model the distribution function in a more efficient can improve the computation speed allowing real-time interactive visualizations.

For clarity and simplicity in introducing the proposed framework, we chose to exclude the consideration of covariance. This framework supports covariance through the utilization of upsampling methods, distance functions, and visualization techniques that take into account the covariance. However, to our knowledge the literature does not offer any upsampling criteria considering the covariance, which can be a future research direction to identify interpolation methods and criteria to consider the covariance. The categorization of distance functions is not contingent on the incorporation of covariance and is therefore universally applicable.

8 Conclusion

This study introduces a theoretical framework designed for the comparison of observations, such as the identification of similarities, differences, or patterns—a challenge routinely encountered by scientists working with uncertain data. The presented techniques empower these scientists to generate comprehensive comparative visualizations for scalar fields with uncertainty in a dense visualization employing the explicit encoding paradigm, thus allowing to quickly identify areas of interest of dis-/similarities. The framework accomplishes this by employing one or more interpolation stages,

incorporating statistical distance functions, and leveraging an appropriate visualization method. Thus, this framework is a good way to discuss comparative uncertainty visualization using the explicit encoding paradigm.

This article defined how methods of different stages can be classified and how those properties influence the comparative visualization. Especially important are the metric properties of the distance functions which mainly influence the resulting visualization and its interpretation. In the presented experiments, we elucidated how to choose methods based on the presented classifications.

The mentioned instances of the framework leave interesting challenges for further investigations for the visualization of uncertain data. Distance functions, which return distributions, create the need for proper visualization methods to present intuitive visualizations. While visualization techniques to visualize individual scalar fields with uncertainty are present, an in-depth analysis for an intuitive way of presenting uncertain similarities or dissimilarities still needs to be done.

A Interpolation

To give the reader an overview about how each upsampling criterion influences the resulting interpolants, Figs. 9, 10, 11 show visualizations of three different interpolation methods. Table 2 shows which interpolation method satisfies which of the following interpolation criteria:

- (i) No additional modes.

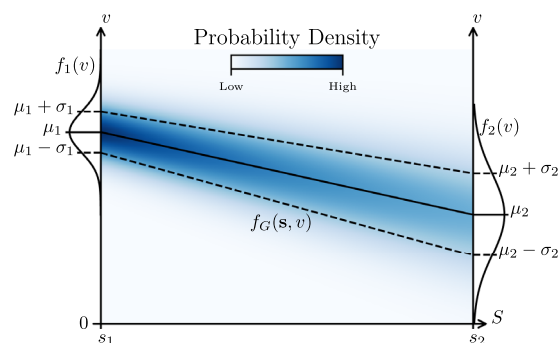


Fig. 9 Given two normal distributions at the observed positions s_1, s_2 , the Gaussian PDF interpolation $f_G(s, v)$ can be computed by interpolating the moments of the normal distributions f_1, f_2

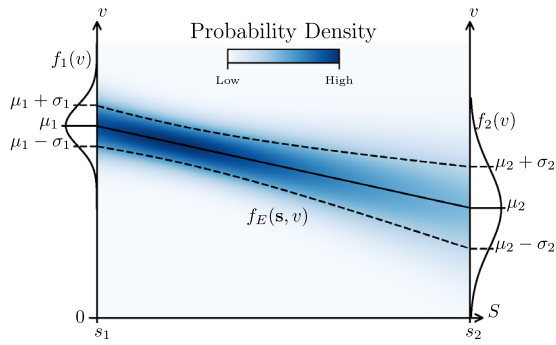


Fig. 10 Given two normal distributions at the observed positions s_1, s_2 , ensemble PDF interpolation draws samples from the distributions X_1, X_2 . These samples are interpolated between the pairs and the interpolant PDFs are calculated. Here, a Gaussian distribution is assumed as interpolant PDFs $f_E(s, v)$

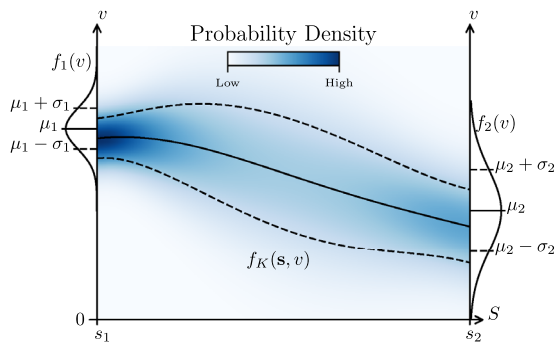


Fig. 11 Given two normal distributions at the observed positions s_1, s_2 , kriging approximates the random variables X_1, X_2 at the grid points using a Gaussian process regression of the multivariate Gaussian distribution $f_K(s, v) \sim \mathcal{N}(\mu(s), \sigma^2(s))$

Table 2 Overview of the exemplary upsampling methods and if the upsampling method satisfies which of the upsampling criteria

	(i)	(ii)	(iii)	(iv)
Gaussian PDF interpolation	✓	✓	✓	
Ensemble PDF interpolation	✓		✓	
Kriging	✓	✓	✓	✓

- (ii) The minimal variance of the interpolants is not smaller than the lowest variance of the interpolated distributions.
- (iii) The interpolants are PDFs.
- (iv) The variance of the interpolants should increase proportional with the distance to a grid point.

B Probabilistic distance function

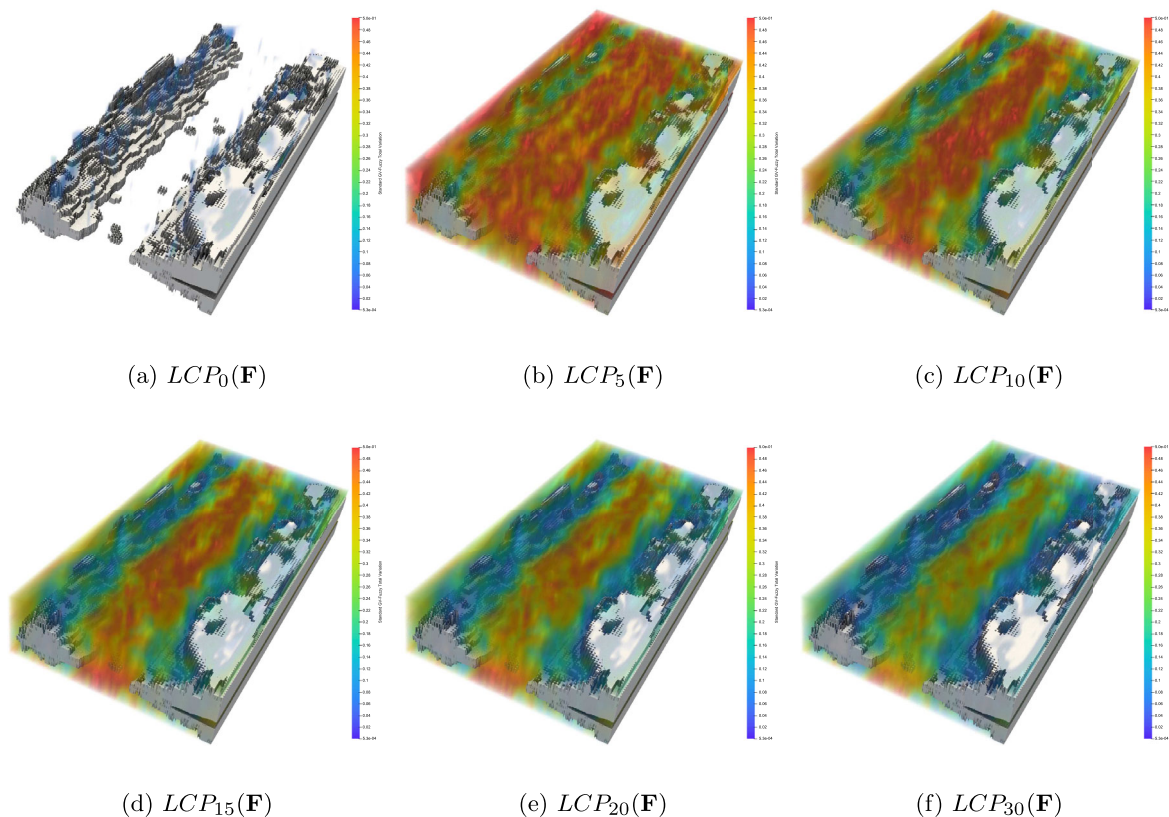


Fig. 12 Direct volume rendering of several LCPs of the probabilistic distance function F . The values x for the LCP of the *difference* F are **a** 0, **b** 5, **c** 10, **d** 15, **e** 20, and **f** 30. In **a**, the probability $LCP_0(F)$ for low differences ($x = 0$) is only visible with a low probability (LCP)

which indicates that the two data sets do not have small differences. This changes rapidly for a higher value $x \geq 5$ **b–f**, while the higher differences $LCP_{x \geq 0}(F)$ mostly occur close to the equator

Author Contributions V.L. wrote the main manuscript text. All authors made substantial contributions to the conception or design of the work.

Funding Open Access funding enabled and organized by Projekt DEAL.

Data availability No datasets were generated or analyzed during the current study.

Declarations

Conflict of interest The authors declare no conflict of interest.

Open Access This article is licensed under a Creative Commons Attribution 4.0 International License, which permits use, sharing, adaptation, distribution and reproduction in any medium or format, as long as you give appropriate credit to the original author(s) and the source, provide a link to the Creative Commons licence, and indicate if changes were made. The images or other third party material in this article are included in the article's Creative Commons licence, unless indicated otherwise in a credit line to the material. If material is not included in the article's Creative Commons licence and your intended use is not permitted by statutory regulation or exceeds the permitted use, you will need to obtain permission directly from the copyright holder. To view a copy of this licence, visit <http://creativecommons.org/licenses/by/4.0/>.

References

1. Athawale, T., Entezari, A.: Uncertainty quantification in linear interpolation for isosurface extraction. *IEEE Trans. Visual. Comput. Gr.* **19**(12), 2723–2732 (2013). <https://doi.org/10.1109/tvcg.2013.208>
2. Athawale, T., Sakhaee, E., Entezari, A.: Isosurface visualization of data with nonparametric models for uncertainty. *IEEE Trans. Visual. Comput. Gr.* **22**(1), 777–786 (2016). <https://doi.org/10.1109/tvcg.2015.2467958>
3. Athawale, T.M., Sane, S., Johnson, C.R.: Uncertainty visualization of the marching squares and marching cubes topology cases. In: *IEEE Visualization Conference (VIS)*. IEEE (2021). <https://doi.org/10.1109/vis49827.2021.9623267>
4. Ayachit, U.: *The ParaView Guide: A Parallel Visualization Application*. Kitware (2015)
5. De Baets, Bernard: Three approaches to the comparison of random variables. In: Ngoc Thach, Nguyen, Kreinovich, Vladik, Trung, Nguyen Duc (eds.) *Data Science for Financial Econometrics*, pp. 93–98. Springer International Publishing, Cham (2021). https://doi.org/10.1007/978-3-030-48853-6_6
6. Bonneau, Georges-Pierre., Hege, Hans-Christian., Johnson, Chris R., Oliveira, Manuel M., Potter, Kristin, Rheingans, Penny, Schultz, Thomas: Overview and state-of-the-art of uncertainty visualization. In: Hansen, Charles D., Chen, Min, Johnson, Christopher R., Kaufman, Arie E., Hagen, Hans (eds.) *Scientific Visualization*:

- Uncertainty, Multifield, Biomedical, and Scalable Visualization, pp. 3–27. Springer London, London (2014). https://doi.org/10.1007/978-1-4471-6497-5_1
7. Brodlić, Ken, Allendes Osorio, Rodolfo, Lopes, Adriano: A review of uncertainty in data visualization. In: Dill, John, Earnshaw, Rae, Kasik, David, Vince, John, Wong, Pak Chung (eds.) *Expanding the Frontiers of Visual Analytics and Visualization*, pp. 81–109. Springer London, London (2012). https://doi.org/10.1007/978-1-4471-2804-5_6
 8. Burago, D., Burago, Y., Ivanov, S.: *A Course in Metric Geometry*, vol. 33. American Mathematical Society, US (2022)
 9. Cha, S.H.: Comprehensive survey on distance/similarity measures between probability density functions. *Int. J. Math. Models Methods Appl. Sci.* **1**(4), 300–307 (2007)
 10. Crissaff, L., Ruby, L.W., Deutch, S., et al.: ARIES: enabling visual exploration and organization of art image collections. *IEEE Comput. Gr. Appl.* **38**(1), 91–108 (2018). <https://doi.org/10.1109/mcg.2017.377152546>
 11. Djurcilov, S., Kim, K., Lermusiaux, P., et al.: Visualizing scalar volumetric data with uncertainty. *Comput. Gr.* **26**(2), 239–248 (2002). [https://doi.org/10.1016/s0097-8493\(02\)00055-9](https://doi.org/10.1016/s0097-8493(02)00055-9)
 12. Eichelbaum, S., Hlawitschka, M., Wiebel, A., et al.: Openwalnut - an open-source visualization system. In: Bengert W, Gerndt A, Su S, et al (eds) *Proceedings of 6th High-End Visualization Workshop*, pp 76–78 (2010)
 13. Gleicher, M., Albers, D., Walker, R., et al.: Visual comparison for information visualization. *Inf. Vis.* **10**(4), 289–309 (2011). <https://doi.org/10.1177/1473871611416549>
 14. Grigorenko, O., Miñana, J.J., Valero, O.: Two new methods to construct fuzzy metrics from metrics. *Fuzzy Sets Syst.* **467**, 108483 (2023). <https://doi.org/10.1016/j.fss.2023.02.004>
 15. Hao, L., Healey, C.G., Bass, S.A.: Effective visualization of temporal ensembles. *IEEE Trans. Visual Comput. Gr.* **22**(1), 787–796 (2016). <https://doi.org/10.1109/tvcg.2015.2468093>
 16. Hoang, D., Klacansky, P., Bhatia, H., et al.: A study of the trade-off between reducing precision and reducing resolution for data analysis and visualization. *IEEE Trans. Visual Comput. Gr.* **25**(1), 1193–1203 (2019). <https://doi.org/10.1109/tvcg.2018.2864853>
 17. Hollister, B.E., Pang, A.: Interpolation of non-gaussian probability distributions for ensemble visualization. *Proc IEEE Vis Posters* (2013)
 18. Hotz, I., Bujack, R., Garth, C., et al.: Mathematical foundations in visualization. In: *Foundations of Data Visualization*. Springer, p 87–119, (2020). https://doi.org/10.1007/978-3-030-34444-3_5
 19. Hummel, M., Jöckel, L., Schäfer, J., et al.: Evaluating sampling strategies for visualizing uncertain multi-phase fluid simulation data. *Appl. Mech. Mater.* **869**, 139–148 (2017). <https://doi.org/10.4028/www.scientific.net/amm.869.139>
 20. Johnson, C., Sanderson, A.: A next step: visualizing errors and uncertainty. *IEEE Comput. Gr. Appl.* **23**(5), 6–10 (2003). <https://doi.org/10.1109/mcg.2003.1231171>
 21. Kamal, A., Dhakal, P., Javaid, A.Y., et al.: Recent advances and challenges in uncertainty visualization: a survey. *J. Visual.* **24**(5), 861–890 (2021). <https://doi.org/10.1007/s12650-021-00755-1>
 22. Kantorovich, L.V.: Mathematical methods of organizing and planning production. *Manag. Sci.* **6**(4), 366–422 (1960). <https://doi.org/10.1287/mnsc.6.4.366>
 23. Kehrer, J., Hauser, H.: Visualization and visual analysis of multifaceted scientific data: a survey. *IEEE Trans. Visual Comput. Gr.* **19**(3), 495–513 (2013). <https://doi.org/10.1109/tvcg.2012.110>
 24. Kim, K., Carlis, J.V., Keefe, D.F.: Comparison techniques utilized in spatial 3d and 4d data visualizations: a survey and future directions. *Comput. Gr.* **67**, 138–147 (2017). <https://doi.org/10.1016/j.cag.2017.05.005>
 25. Knoll, A., Hijazi, Y., Kensler, A., et al.: Fast ray tracing of arbitrary implicit surfaces with interval and affine arithmetic. *Comput. Gr. Forum* **28**(1), 26–40 (2009). <https://doi.org/10.1111/j.1467-8659.2008.01189.x>
 26. Köthür, P., Witt, C., Sips, M., et al.: Visual analytics for correlation-based comparison of time series ensembles. *Comput. Gr. Forum* **34**(3), 411–420 (2015). <https://doi.org/10.1111/cgf.12653>
 27. Kramosil, I., Michálek, J.: Fuzzy metrics and statistical metric spaces. *Kybernetika* **11**(5), 336–344 (1975)
 28. Krueger, R., Sun, G., Beck, F., et al.: TravelDiff: Visual comparison analytics for massive movement patterns derived from twitter. In 2016 IEEE Pacific Visualization Symposium (PacificVis). IEEE (2016). <https://doi.org/10.1109/pacificvis.2016.7465266>
 29. Lee, C.H., Gutierrez, F., Dou, D.: Calculating feature weights in naive bayes with kullback-leibler measure. In: 2011 IEEE 11th International Conference on Data Mining. IEE (2011). <https://doi.org/10.1109/icdm.2011.29>
 30. Li, J., Heap, A.D.: A review of spatial interpolation methods for environmental scientists. *Geoscience Australia, Canberra* pp 137–145 (2008)
 31. Liu, S., Levine, J.A., Bremer, P., et al.: Gaussian mixture model based volume visualization. In: *IEEE Symposium on Large Data Analysis and Visualization (LDVAV)*. IEEE (2012). <https://doi.org/10.1109/ldav.2012.6378978>
 32. LYI, S., Jo, J., Seo, J.: Comparative layouts revisited: design space, guidelines, and future directions. *IEEE Trans. Visual Comput. Gr.* **27**(2), 1525–1535 (2021). <https://doi.org/10.1109/tvcg.2020.3030419>
 33. Menger, Karl: *Statistical Metrics*. In: Menger, Karl, Schweizer, Bert, Sklar, Abe, Sigmund, Karl, Gruber, Peter, Hlawka, Edmund, Reich, Ludwig, Schmetterer, Leopold (eds.) *Selecta Mathematica: Volume 2*, pp. 433–435. Springer Vienna, Vienna (2011). https://doi.org/10.1007/978-3-7091-6045-9_35
 34. Musleh, M., Muren, L.P., Toussaint, L., et al.: Uncertainty guidance in proton therapy planning visualization. *Comput. Gr.* **111**, 166–179 (2023). <https://doi.org/10.1016/j.cag.2023.02.002>
 35. Myers, D.E.: Spatial interpolation: an overview. *Geoderma* **62**(1–3), 17–28 (1994). [https://doi.org/10.1016/0016-7061\(94\)90025-6](https://doi.org/10.1016/0016-7061(94)90025-6)
 36. Obermaier, Harald, Bensema, Kevin, Joy, Kenneth I.: Visual trends analysis in time-varying ensembles. *IEEE Trans. Visual. Comput. Gr.* **22**(10), 2331–2342 (2016). <https://doi.org/10.1109/TVCG.2015.2507592>
 37. Palmer, T.N., Alessandri, A., Andersen, U., et al.: Development of a European multimodel ensemble system for seasonal-to-interannual prediction (DEMETER). *Bull. Am. Meteor. Soc.* **85**(6), 853–872 (2004). <https://doi.org/10.1175/BAMS-85-6-853>
 38. Pang, A.T., Wittenbrink, C.M., Lodha, S.K.: Approaches to uncertainty visualization. *Vis. Comput.* **13**(8), 370–390 (1997)
 39. Pfaffelmoser, T., Reitingger, M., Westermann, R.: Visualizing the positional and geometrical variability of isosurfaces in uncertain scalar fields. *Comput. Gr. Forum* **30**(3), 951–960 (2011). <https://doi.org/10.1111/j.1467-8659.2011.01944.x>
 40. Pöthkow, K., Hege, H.C.: Positional uncertainty of isocontours: condition analysis and probabilistic measures. *IEEE Trans. Visual Comput. Gr.* **17**(10), 1393–1406 (2011). <https://doi.org/10.1109/tvcg.2010.247>
 41. Pöthkow, K., Hege, H.C.: Nonparametric models for uncertainty visualization. *Comput. Gr. Forum* **32**(3pt2), 131–140 (2013). <https://doi.org/10.1111/cgf.12100>
 42. Pöthkow, K., Weber, B., Hege, H.C.: Probabilistic marching cubes. *Comput. Gr. Forum* **30**(3), 931–940 (2011). <https://doi.org/10.1111/j.1467-8659.2011.01942.x>
 43. Rautenhaus, Marc, Bottinger, Michael, Siemen, Stephan, Hoffman, Robert, Kirby, Robert M., Mirzargar, Mahsa, Rober, Niklas, Westermann, Rudiger: Visualization in meteorology—a survey of techniques and tools for data analysis tasks. *IEEE Trans. Visual. Comput. Gr.* **24**(12), 3268–3296 (2018). <https://doi.org/10.1109/TVCG.2017.2779501>

44. Repovš, G., Barch, D.M.: Working memory related brain network connectivity in individuals with schizophrenia and their siblings. *Front. Hum. Neurosci.* (2012). <https://doi.org/10.3389/fnhum.2012.00137>
45. Repovš, Grega, Csernansky, John G., Barch, Deanna M.: Brain network connectivity in individuals with schizophrenia and their siblings. *Biol. Psychiatry* **69**(10), 967–973 (2011). <https://doi.org/10.1016/j.biopsych.2010.11.009>
46. Rubner, Y., Tomasi, C., Guibas, L.: A metric for distributions with applications to image databases. In: Sixth International Conference on Computer Vision (IEEE Cat. No.98CH36271). Narosa Publishing House, (1998). <https://doi.org/10.1109/iccv.1998.710701>
47. Sakhæe, E., Entezari, A.: A statistical direct volume rendering framework for visualization of uncertain data. *IEEE Trans. Visual Comput. Gr.* **23**(12), 2509–2520 (2017). <https://doi.org/10.1109/tvcg.2016.2637333>
48. Sane, S., Athawale, T.M., Johnson, C.R.: Visualization of uncertain multivariate data via feature confidence level-sets. *EuroVis 2021 - Short Papers* (2021). <https://doi.org/10.2312/EVS.20211053>
49. Schlegel, S., Korn, N., Scheuermann, G.: On the interpolation of data with normally distributed uncertainty for visualization. *IEEE Trans. Visual Comput. Gr.* **18**(12), 2305–2314 (2012). <https://doi.org/10.1109/tvcg.2012.249>
50. Schweizer, B., Sklar, A.: Statistical metric spaces. *Pac. J. Math.* **10**(1), 313–334 (1960)
51. Schweizer, B., Sklar, A.: Probabilistic metric spaces. *North Holland series in probability and applied mathematics*, Elsevier Science, London, England (1983)
52. Shu, Q., Guo, H., Liang, J., et al.: EnsembleGraph: Interactive visual analysis of spatiotemporal behaviors in ensemble simulation data. In: 2016 IEEE Pacific Visualization Symposium (PacificVis). IEEE (2016). <https://doi.org/10.1109/pacificvis.2016.7465251>
53. Siddiqui, F., Höllt, T., Vilanova, A.: A progressive approach for uncertainty visualization in diffusion tensor imaging. *Comput. Gr. Forum* **40**(3), 411–422 (2021). <https://doi.org/10.1111/cgf.14317>
54. Srinivasan, A., Brehmer, M., Lee, B., et al.: What's the difference? In: Proceedings of the 2018 CHI Conference on Human Factors in Computing Systems. ACM (2018). <https://doi.org/10.1145/3173574.3173878>
55. Telea, A.C.: *Data Visualization—Principles and Practice*, 2nd edn. CRC Press, Boca Raton, Fla (2014)
56. Vietinghoff, D., Böttinger, M., Scheuermann, G., et al.: A mathematical foundation for the spatial uncertainty of critical points in probabilistic scalar fields. In: 2023 Topological Data Analysis and Visualization (TopoInVis). IEE (2023). <https://doi.org/10.1109/topoinvis60193.2023.00010>
57. Wang, J., Hazarika, S., Li, C., et al.: Visualization and visual analysis of ensemble data: a survey. *IEEE Trans. Visual Comput. Gr.* **25**(9), 2853–2872 (2019). <https://doi.org/10.1109/tvcg.2018.2853721>



Viktor Leonhardt is a PhD student at the computer science department of the Rheinland-Pfälzische Technische Universität Kaiserslautern-Landau. He received his Bachelor of Science (B.Sc) and Master of Science (M.Sc) in Computer Science from the Technische Universität Kaiserslautern. His research interests include comparative uncertainty visualization and artificial intelligence, with a focus on graph convolution neural networks.



Alexander Wiebel is professor of visual computing at Hochschule Worms University of Applied Sciences in Germany. He received his Ph.D. degree from Universität Leipzig in 2008 and has been a postdoctoral researcher at Max Planck Institute for Human Cognitive and Brain Sciences, and later at Zuse Institute Berlin (ZIB). Between 2013 and 2015, he was a professor at Hochschule Coburg. His research interests include visual data analysis and its applications as well as virtual and augmented

reality.



Christoph Garth received the PhD degree in computer science from Technische Universität (TU) Kaiserslautern in 2007. After four years as a postdoctoral researcher with the University of California, Davis, he rejoined TU Kaiserslautern where he is currently a full professor of computer science. His research interests include large-scale data analysis and visualization, in situ visualization, topology-based methods, and interdisciplinary applications of visualization.

Publisher's Note Springer Nature remains neutral with regard to jurisdictional claims in published maps and institutional affiliations.